Kinetics of superoxide reactions with dissolved organic matter in tropical Atlantic surface waters near Cape Verde (TENATSO)

M. I. Heller[1] and P. L. Croot[1]

[1]   The decay kinetics of superoxide (O_2^-) reacting with organic matter was examined in oligotrophic waters at, and nearby, the TENATSO ocean observatory adjacent to the Cape Verde archipelago. Superoxide is the short-lived primary photochemical product of colored dissolved organic matter (CDOM) photolysis and also reacts with CDOM or trace metals (Cu, Fe) to form H_2O_2. In the present work we focused our investigations on reactions between CDOM and superoxide. O_2^- decay kinetics experiments were performed by adding KO_2 to diethylenetriaminepentaacetic acid (DTPA) amended seawater and utilizing an established chemiluminescence technique for the detection of O_2^- at nM levels. In Cape Verdean waters we found a significant reactivity of superoxide with CDOM with maximal rates adjacent to the chlorophyll maximum, presumably from production of new CDOM from bacteria/phytoplankton. This work highlights a poorly understood process which impacts on the biogeochemical cycling of CDOM and trace metals in the open ocean.

Citation: Heller, M. I., and P. L. Croot (2010), Kinetics of superoxide reactions with dissolved organic matter in tropical Atlantic surface waters near Cape Verde (TENATSO), *J. Geophys. Res.*, *115*, C12038, doi:10.1029/2009JC006021.

1.   Introduction

[2]   The superoxide (O_2^-) radical is suspected to be a critically important species involved in the redox cycling of metal ions in natural waters [*Heller and Croot*, 2010a; *Rose and Waite*, 2006; *Voelker et al.*, 2000]. In sunlit surface waters O_2^- is a major product of the photooxidation of colored dissolved organic matter (CDOM) [*Micinski et al.*, 1993; *O'Sullivan et al.*, 2005] and it can also be produced via phytoplankton metabolic processes [*Marshall et al.*, 2005]. Inorganic and organic complexes of Cu(II)/Cu(I) and Fe(II)/Fe(III) can react rapidly with superoxide leading to a catalytic cycle for superoxide decay [*Voelker et al.*, 2000]. The products of superoxide decomposition are H_2O_2 and O_2, and photochemically produced superoxide is believed to be the major pathway for H_2O_2 formation in the ocean [*Croot et al.*, 2004; *O'Sullivan et al.*, 2005; *Yuan and Shiller*, 2001]. There is currently a lack of published data on direct measurements of superoxide production rates from the open ocean, with only a recent study on nonphotochemical production [*Rose et al.*, 2008] and an earlier study investigating photoproduction in the Caribbean [*Micinski et al.*, 1993] available. In the absence of direct measurements, H_2O_2 photoproduction rates can be used as a reasonable estimate of the major O_2^- source in the ocean [*Zafiriou*, 1990]. A number of reactions have been identified in seawater that affect superoxide decay rates and these include the following: (1) the second-order uncatalyzed dismutation

reaction of superoxide with its conjugate acid (HO_2) [*Zafiriou*, 1990], (2) reactions with Cu species in seawater [*Voelker et al.*, 2000], (3) reactions with Fe species in seawater [*Rose and Waite*, 2006], and (4) reactions with CDOM [*Goldstone and Voelker*, 2000]. Overall the kinetic reactivity of O_2^- is then determined by the following reactions:

$$\frac{\partial [O_2^-]}{\partial t} = 2k_2 [O_2^-]^2 + \sum k_M [M]_X [O_2^-] + k_{org} [O_2^-] \quad (1)$$

where k_2 is the second-order uncatalyzed dismutation rate constant, $[M]_X$ denotes the concentration of different metal species, and (k_M) is the rate constants for the reactions with metals and includes both the Cu(II)/Cu(I) and Fe(III)/Fe(II) redox pairs (see below), the reaction with organic substances is described by the first-order rate k_{org}.

$$\sum k_M [M]_X = \big(k_{Cu(I)}[Cu(I)] + k_{Cu(II)}[Cu(II)] + k_{Fe(II)}[Fe(II)] \\ + k_{Fe(III)}[Fe(III)] \big) \quad (2)$$

The observed rate of superoxide decay can then be written as follows with only a single term each for the first-order and second-order rate components

$$\frac{\partial [O_2^-]}{\partial t} = -2k_2 [O_2^-]^2 - k_{obs} [O_2^-] \quad (3)$$
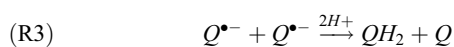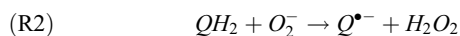
where k_{obs} is described as the sum of the first-order reaction rates.

$$k_{obs} = \sum k_M [M]_X + k_{org} \quad (4)$$

---

[1]FB2 Marine Biogeochemie, Leibniz-Institut für Meereswissenschaften, Dienstgebäude Westufer, Kiel, Germany.

Metal complexes of the chelator diethylenetriaminepenta-acetic acid (DTPA) react only very slowly with superoxide and so under the conditions of sufficient DTPA to complex reactive trace metals it can be assumed that $k_{obs} = k_{org}$ [*Goldstone and Voelker*, 2000].

[3] CDOM is the main light absorbing substance in the ocean and represents an important chromophore in the UV region. CDOM plays an important role in light availability for primary productivity [*Blough and Del Vecchio*, 2002] and for photochemical reactions where it is critical to the production of free radical species [*Dister and Zafiriou*, 1993]. In the open ocean CDOM is produced by hetero-trophic processes in the upper water column [*Steinberg et al.*, 2004] and is destroyed by solar bleaching. Key components identified in CDOM include humic and fulvic acids which can also form complexes with trace metals [*Cory and McKnight*, 2005]. The redox active fraction of CDOM, which can easily exchange electrons, has been attributed to quinone moieties [*Scott et al.*, 1998]. Quinones can shuttle between three redox states; the fully oxidized quinone (Q), which can undergo a one electron reduction to the semiquinone radical ($Q^{\bullet-}$) and with a further one electron reduction to the hydroquinone (QH_2). Superoxide reacts rapidly with both the quinone and hydroquinone to form the radical semiquinone species [*Shkarina et al.*, 2001], which dismutates to reform the starting quinone and hydroquinone, thus creating a potential catalytic cycle for the decay of superoxide [*Goldstone and Voelker*, 2000]. H_2O_2 is also produced from the superoxide mediated oxidation of the hydroquinone [*Ishii and Fridovich*, 1990].

(R1) $$Q + O_2^- \rightarrow Q^{\bullet-} + O_2$$

(R2) $$QH_2 + O_2^- \rightarrow Q^{\bullet-} + H_2O_2$$

(R3) $$Q^{\bullet-} + Q^{\bullet-} \xrightarrow{2H+} QH_2 + Q$$

where Q is the quinone, QH_2 is the hydroquinone and $Q^{\bullet-}$ is the semiquinone radical [*Eyer*, 1991; *Roginsky et al.*, 1999]. It should be noted that for reaction (R3) there is no pH dependence as H^+ is not a reactant in the rate limiting step. The initial reaction is to form the quinone and the un-protonated hydroquinone. The pKa's of hydroquinone are both above pH 8 (pKa$_1$ = 9.6–10, pKa$_2$ = 11.4–11.9 [*Eyer*, 1991] and thus at seawater pH the hydroquinone is expected to be in the QH_2 form. As pointed out by *Meisel* [1975] for reaction (R3) at pH's below 10 the initially formed Q^{2-} will rapidly protonate to form QH_2 and thus in seawater the influence of pH is not important on this reaction. The pKa for the semiquinone is 4.1 [*Eyer*, 1991] and thus the de-protonated species dominates at seawater pH. The semi-quinone radical however can also generate superoxide by reactions with oxygen [*Meisel*, 1975].

(R4) $$Q^{\bullet-} + O_2 \rightarrow Q + O_2^-$$
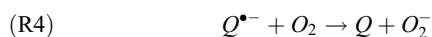
The overall aim of our study is to assess the role of super-oxide in iron redox cycling and its potential for aiding the dissolution of Saharan aerosols deposited in the tropical Atlantic. In this present work we examine the organic (nonmetal) pathways for superoxide decay in seawater in order to better understand other key pathways for superox-ide loss in seawater. This is the first study that we are aware of in open ocean waters that focuses on the relationship between CDOM and the organic reactions with superoxide in seawater.

2. Methodology

2.1. Chemical Analysis

2.1.1. Reagents

[4] All reagents were prepared using 18MΩ cm resistivity water (hereafter MQ water) supplied by a combination of an ELIX-3 and Synergy 185 water systems (Millipore). MCLA ([2-methyl-6-(4-methoxyphenyl)-3,7-dihydroimidazo[1,2-a]pyrazin-3-one, HCl]), (Fluka) was used as received. A primary 1 mM MCLA standard, was prepared by dissolving 10 mg MCLA in 34.5 mL MQ water. Aliquots (1 mL) of the primary solution were then pipetted into polyethylene vials and frozen at −80°C until required for use. The working MCLA standard, 1 μM, was prepared from a thawed vial of the primary stock by dilution into 1 L MQ water. This solution was buffered in 0.05 M sodium acetate and adjusted to pH$_{NBS}$ of 6 with quartz distilled 6 M HCl (Q-HCl). A 3.8 mM stock solution of DTPA was made up by dissolving 0.6g in 400 mL MQ water. For each experiment a fresh superoxide stock was provided in a dark glass bottle by adding a specific amount (8–10 mg) of potassium super-oxide, KO$_2$ (As a powder purchased from Aldrich, product number 278904), to a pH$_{NBS}$ = 13 NaOH solution. This pH ensured a stable superoxide concentration over the required experiment time. All plasticware used in this work was extensively acid cleaned before use with 0.1 M Q-HCl.

2.1.2. Measurement of Sample pH

[5] In the present manuscript we report seawater pH values using the total hydrogen scale (pH$_{TOT}$) [*Dickson*, 1993] while we use the NBS scale (pH$_{NBS}$) for pH mea-surements of buffers and other low ionic strength solutions. All pH measurements during the course of this work were made using a WTW 330i pH meter calibrated with Tris buffers [*Millero et al.*, 1993].

2.1.3. Seawater Sampling

[6] During May 2009 we occupied three stations in the vicinity of the island of Sao Vicente in the Cape Verde archipelago (see Figure 1): Station 8 (S8) to the North East on 17 May (17°20′N 24°47′W), Station 9 (S9) to the southwest on 23 May (16°44′N 25°15′W), and Station 10 (S10) on 30 May at the TENATSO time series observatory (17°35′N 24°15′W). At each station we obtained continuous vertical profiles for temperature, salinity and oxygen. Dis-crete samples were obtained for chlorophyll, CDOM and superoxide decay kinetics (Table 1). Macronutrients and H$_2O_2$ during May 2009 were only sampled at the TENATSO site, which had also previously been sampled for these parameters in November 2008. Sampling was performed using a CTD-rosette (Seabird) sampling system deployed from the R/V *Islandia* (INDP, Cape Verde). Discrete sam-ples were taken using 8 L Niskin Bottles on the 12 bottle rosette. Samples for macronutrients and chlorophyll were analyzed using standard protocols [*Grasshoff et al.*, 1999].

2.1.4. CDOM Measurements

[7] CDOM measurements were performed using a LWCC-2100 100 cm path length liquid waveguide cell
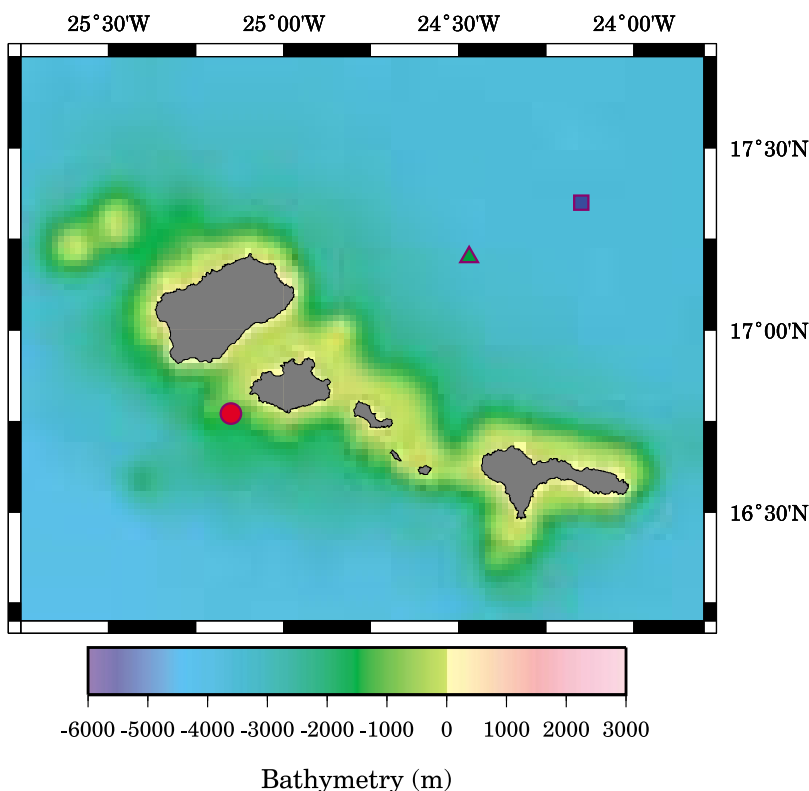
Figure 1. Location of the sampling stations referred to in the text. Station 8 (S8) is shown as a green triangle, Station 9 (S9) is a red circle, and Station 10 (S10 TENATSO) is depicted as a blue square.

(World Precision Instruments, Sarasota, Florida) and an Ocean Optics USB4000 UV-VIS spectrophotometer in conjunction with an Ocean Optics DT-MINI2-GS light source. Samples were syringe filtered through 0.2 μm filters (Sarstedt), the first 10 mL were discarded and the absorbance measured by direct injection into the LWCC. Absorbance measurements were made relative to MQ water and corrected for the refractive index of seawater based on the procedure outlined by *Nelson et al.* [2007]. The resulting dimensionless optical density spectra were converted to absorption coefficient (m^{-1}): $a_{\text{CDOM}(\lambda)} = 2.303 \, A\lambda / \ell$, where 2.303 converts decadal logarithmic absorbance to base e, and ℓ is the effective optical path length of the waveguide (here 103.8 $\pm$ 0.5 cm as determined by the manufacturer).

2.1.5. H$_2$O$_2$ Measurements in Surface Waters

[8] Samples for H$_2$O$_2$ were analyzed at sea within 1–2 h of collection using a flow injection chemiluminescence (FIA-CL) reagent injection method [*Yuan and Shiller*, 1999] as described previously [*Croot et al.*, 2004]. In brief, the chemiluminescence of luminol is catalyzed by the reaction of H$_2$O$_2$ present in the sample with Co^{2+} at alkaline pH. Samples were analyzed using 5 replicates: typical precision was 2–3% through the concentration range 1–300 nM, the detection limit (3 σ) is typically 0.2 nM.

2.1.6. Superoxide Measurement Technique and Apparatus

[9] For this work, we employed a chemiluminescence analysis method for superoxide utilizing MCLA that has been described previously [*Heller and Croot*, 2010a; *Heller and Croot*, 2010b]. Our system utilizes a commercially available FeLume (Wateville Analytical) system, which is composed of a light tight box equipped with a Plexiglas spiral flow cell mounted below a photon counter (Hamamatsu HC135–01). The photon counter is linked via a Bluetooth serial port to a laptop computer and controlled through a purpose built Labview$^{\text{TM}}$ (National Instruments) virtual instrument. The photon counter has a base counting period of 10 ms, for the present work we used average counts of an integration time of 200 ms. Dark background counts for this detector were typically 60–120 counts s^{-1}. For O$_2^-$ determination we ran the sample and the MCLA reagent directly into the flow cell using a peristaltic pump (Gilson Minipuls 3, operating at 18 rpm,) with the sample line being pulled through the flow cell as this leads to the smallest amount of dead time in the system (typically 2–3 s). The overall flow rate through the cell was 8.25 mL min^{-1}, comprising 5.0 mL min^{-1} from the MCLA and 3.25 mL min^{-1} from the sample. The transit time through the optical cell (300 μL) was therefore 2.18 s. All experiments were performed at 23.0 $\pm$ 0.1°C in a Class 5 clean room with both samples and reagents maintained at this temperature as the MCLA sensitivity for superoxide is temperature-dependent [*Heller and Croot*, 2010b].

2.1.7. Field Measurements of Superoxide Reaction Rates in Seawater

[10] Our approach is based on measuring the decay rate of known quantities of added O$_2^-$ (as KO$_2$) to seawater. O$_2^-$ is detected via its chemiluminescence reaction with MCLA. The experimental setup used here was the same as we had used previously [*Heller and Croot*, 2010a] but in this case

Table 1. Superoxide Decay Kinetics and aCDOM(300 nm) Measured During This Study

Station	Depth (m)	First Order Fit	First and Second Order Fit		aCDOM (m^{-1})
		k_{org} (s^{-1})[a]	k_1 (s^{-1})	k_2 (M^{-1} s^{-1})	
S08	10	-0.0093 ± 0.0002	-0.0093 ± 0.0004	$4.0 \pm 1.4 \times 10^4$	0.364
S08	20	-0.0158 ± 0.0004	-0.0158 ± 0.0028	$1.3 \pm 0.7 \times 10^5$	0.391
S08	30	-0.0147 ± 0.0002	-0.0147 ± 0.0010	$5.8 \pm 2.7 \times 10^4$	0.415
S08	40	-0.0138 ± 0.0002	-0.0138 ± 0.0009	$5.6 \pm 3.3 \times 10^4$	0.428
S08	60	-0.0134 ± 0.0002	-0.0134 ± 0.0009	$4.6 \pm 3.1 \times 10^4$	0.433
S08	70	-0.0133 ± 0.0002	-0.0133 ± 0.0006	$3.5 \pm 2.1 \times 10^4$	0.417
S08	80	-0.0119 ± 0.0003	-0.0119 ± 0.0012	$6.0 \pm 3.2 \times 10^4$	0.337
S08	100	-0.0125 ± 0.0002	-0.0125 ± 0.0011	$8.0 \pm 3.6 \times 10^4$	0.444
S08	150	-0.0116 ± 0.0003	-0.0116 ± 0.0016	$7.5 \pm 4.4 \times 10^4$	0.293
S08	200	-0.0155 ± 0.0004	-0.0155 ± 0.0019	$1.0 \pm 6.2 \times 10^5$	0.377
S08	300	-0.0137 ± 0.0003	-0.0137 ± 0.0010	$6.5 \pm 3.2 \times 10^4$	0.368
S08	400	-0.0153 ± 0.0004	-0.0153 ± 0.0012	$9.0 \pm 4.4 \times 10^4$	0.297
S09	10	-0.0156 ± 0.0002	-0.0156 ± 0.0006	$1.7 \pm 4.2 \times 10^4$	0.308
S09	20	-0.0133 ± 0.0002	-0.0133 ± 0.0009	$1.7 \pm 8.2 \times 10^4$	0.158
S09	30	-0.0123 ± 0.0002	-0.0123 ± 0.0004	$1.3 \pm 2.2 \times 10^4$	0.240
S09	40	-0.0175 ± 0.0002	-0.0175 ± 0.0006	$1.0 \pm 4.6 \times 10^4$	0.308
S09	60	-0.0190 ± 0.0004[b]	-0.0190 ± 0.0057[b]	$3.3 \pm 5.1 \times 10^5$	0.411
S09	70	-0.0342 ± 0.0011[b]	-0.0342 ± 0.0035[b]	$3.3 \pm 2.8 \times 10^5$	0.455
S09	80	-0.0321 ± 0.0005[b]	-0.0321 ± 0.0015[b]	$1.3 \pm 1.3 \times 10^5$	0.668
S09	100	-0.0325 ± 0.0006[b]	-0.0325 ± 0.0013[b]	$1.5 \pm 1.4 \times 10^5$	0.311
S09	150	-0.0256 ± 0.0002[b]	-0.0256 ± 0.0008[b]	$7.5 \pm 9.6 \times 10^4$	0.304
S09	200	-0.0266 ± 0.0003	-0.0266 ± 0.0006	$9.2 \pm 7.7 \times 10^4$	0.277
S09	300	-0.0162 ± 0.0002	-0.0162 ± 0.0005	$7.5 \pm 6.8 \times 10^4$	0.260
S09	400	-0.0142 ± 0.0002	-0.0142 ± 0.0004	$1.3 \pm 0.7 \times 10^5$	0.413
S10	5	-0.0147 ± 0.0002	-0.0147 ± 0.0002	$1.4 \pm 1.1 \times 10^4$	0.497
S10	10	-0.0129 ± 0.0003	-0.0129 ± 0.0005	$4.6 \pm 3.4 \times 10^4$	0.482
S10	20	-0.0133 ± 0.0004	-0.0133 ± 0.0006	$5.0 \pm 2.4 \times 10^4$	0.497
S10	30	-0.0130 ± 0.0002	-0.0130 ± 0.0004	$6.9 \pm 2.5 \times 10^4$	0.495
S10	40	-0.0151 ± 0.0002	-0.0151 ± 0.0004	$7.5 \pm 2.7 \times 10^4$	0.477
S10	50	-0.0168 ± 0.0002	-0.0168 ± 0.0005	$2.5 \pm 3.0 \times 10^4$	0.533
S10	60	-0.0199 ± 0.0017	-0.0199 ± 0.0013	$0.6 \pm 1.8 \times 10^5$	0.581
S10	80	-0.0145 ± 0.0004	-0.0145 ± 0.0019	$3.8 \pm 2.1 \times 10^5$	0.797
S10	100	-0.0179 ± 0.0002	-0.0179 ± 0.0007	$2.3 \pm 0.6 \times 10^5$	0.586
S10	120	-0.0151 ± 0.0002	-0.0151 ± 0.0005	$1.6 \pm 0.6 \times 10^5$	0.553
S10	150	-0.0123 ± 0.0005	-0.0123 ± 0.0020	$0.3 \pm 1.9 \times 10^5$	0.548
S10	200	-0.0153 ± 0.0015	-0.0153 ± 0.0007	$0.8 \pm 1.1 \times 10^5$	0.655

[a]All errors are reported to the 95% confidence interval. The error in aCDOM is ±0.004 at the 95% confidence interval.

[b]Data displayed an initial fast decay rate and a slower secondary rate; the initial rate is reported here. Data were calculated over the initial linear section of a semilog plot of the raw data.

consisted of only the sample treatments with DTPA in order to prevent reactions with trace metals from occurring.

[11] For each experiment up to 10 depths from throughout the water column were sampled. From each depth a 60 mL Teflon bottle was filled with 40 mL of the fresh collected filtered seawater and spiked with DTPA (3.8 μM final concentration). Samples with DTPA were left overnight (12 h) to equilibrate before the addition of superoxide, as we had previously found that shorter equilibration times did not completely remove the influence of the metal ions. After equilibration 20 μL of a freshly prepared KO_2 solution (~100 μM O_2^-) was added to the samples and immediately injected in the flow injection system where the chemiluminescence signal was detected and followed for up to 3 min. The superoxide concentrations of the KO_2 standard was checked by UV spectrophotometry with the same 100 cm long path as used for the CDOM measurements (above) and the concentration of superoxide was calculated by solving for both the superoxide and H_2O_2 absorbance for multiple wavelengths in the range 250–300 nm. Values for the molar absorptivity for O_2^- [*Bielski et al.*, 1985] and HO_2^- [*Bielski and Allen*, 1977] at pH 12.5 were obtained from the relevant literature.

2.1.8. Background Chemiluminescence

[12] MCLA produces chemiluminescence by itself because of autoxidation of the conjugate base of MCLA with O_2 [*Fujimori et al.*, 1993]. Autoxidation reactions are reduced by using an analytical pH less than the pKa of MCLA (7.75) [*Fujimori et al.*, 1998] and by reducing the MCLA concentration [*Kambayashi and Ogino*, 2003]. MCLA also reacts rapidly with singlet oxygen to produce chemiluminescence [*Fujimori et al.*, 1998] however singlet oxygen is present at low pM concentrations as it is efficiently quenched in seawater [*Cory et al.*, 2008]. MCLA also does not appreciably react with H_2O_2 [*Kambayashi and Ogino*, 2003] to produce chemiluminescence at the concentrations encountered (nM to μM) in the present work. In our study we ran seawater samples without added superoxide to determine the baseline chemiluminescence because of the autoxidation reaction of MCLA. The baseline values determined in this manner (range: 7000–15000 counts per 200 ms period) were subtracted from the superoxide decay data in order to correctly determine the decay rate (see below). In the present work where we added nM superoxide in order to observe the decay the baseline corrections were relatively minor with regard to the initial counts (<1%). At lower

concentrations of superoxide baseline correction is more important as is the signal-to-noise ratio. In the present work we convert the raw signal counts into superoxide concentrations using the following relationship:

$$[O_2^-] = \frac{(X - X_b)}{S} \qquad (5)$$

where X is the raw count rate, X_b is the MCLA background chemiluminescence and S the linear sensitivity factor derived from the calibration experiments (see below).

2.1.9. Linearity of the MCLA Technique

[13] We have previously shown [*Heller and Croot*, 2010a] that the chemiluminescence response between MCLA and superoxide is linear over the range of superoxide concentrations employed in this work. The assessment of this linear response is of course complicated by the rapid decay of the superoxide. Previously we performed a series of experiments in which seawater samples were spiked with varying amounts of a known concentration of superoxide and then calculated the initial superoxide signal based on the decay curve. For the configuration used in our experiments we found a linear response, for the range 0–90 nM superoxide, as has been shown previously [*Mitani et al.*, 1994; *Zheng et al.*, 2003]. A practical concern however is that with high concentrations of superoxide (>90 nM) the 1 μM MCLA is insufficient to prevent uncatalyzed dismutation of superoxide in the pH$_{NBS}$ 6 buffer despite the fast reactivity of MCLA with O_2^- [*Akutsu et al.*, 1995; *Gotoh and Niki*, 1990]. An additional check on the linearity of the response was that the calculated rates in DTPA amended seawater [*Heller and Croot*, 2010a] were not significantly different from earlier estimates [*Zafiriou*, 1990]. This would not have been observed if the response was significantly nonlinear. The sensitivity (S in counts per nM superoxide, see above) of the MCLA response for superoxide, can also be assessed in each sample by a variation of equation (6) [*Heller and Croot*, 2010a], and was found to only vary slightly (2–3%) within sample runs using the open ocean samples measured in this work.

2.1.10. Precision and Accuracy

[14] Analysis of replicate samples using near surface water collected from close to Cape Verde, were used to assess the precision of the technique. For this small data set (n = 5), k_{obs} = 0.0245 ± 0.0016 (2σ) indicating a precision of 6.4% for these samples. The main problem associated with this technique initially was the formation of bubbles in the flow cell which gave rise to signal spikes, this problem was reduced when seawater samples were given adequate time to come into equilibrium with the laboratory temperature after collection. Care is also needed in mixing the samples thoroughly when adding the superoxide. For the work reported here from Cape Verde samples were run in duplicate.

[15] The accuracy of the MCLA method for the determination of both superoxide concentration and the value of the rate constants k_1 and k_2 are difficult to assess given that the superoxide concentration is transient and there are no standard reference materials available with a certified rate constant. Direct comparison with the earlier work by Goldstone and Voelker [*Goldstone and Voelker*, 2000] on k_{org} (0.1–1.4 s^{-1}) is also not possible. As their work was

performed using samples at a pH of 9.5 and with significantly higher $a_{CDOM(300)}$ values (0.5–20 m^{-1}) than in our work. In the current work we found good agreement for the pH-dependent value of k_2 (our value: 4.7 ± 2.6 × 10^{12} [H$^+$] M^{-1} s^{-1}:pH$_{TOT}$ scale, n = 30, 95% CI) with our earlier work (4.4 ± 1.6 × 10^{12} [H$^+$] M^{-1} s^{-1}) from low DOM waters in the Southern Ocean [*Heller and Croot*, 2010a] and that of Zafiriou using spectrophotometry [*Zafiriou et al.*, 1998] k_2 (5 ± 1 × 10^{12} [H$^+$] M^{-1} s^{-1}:pH$_{NBS}$ scale). Recently we have shown that the MCLA technique is highly accurate in seawater when calibrated as described here [*Heller and Croot*, 2010b].

2.1.11. Measurement of Impurities in Superoxide Standards Prepared From KO$_2$ and Calibration of the Initial Superoxide Concentration

[16] 1. In the last decades KO$_2$ has not been used widely as a source of superoxide because of the perception that it was highly contaminated with metals. However, it now appears that many of the problems, reported in earlier studies, with KO$_2$ may have resulted from non trace metal clean equipment, most likely from water supplies which did not utilize final filtration as was alluded to in some earlier works [*Weinstein and Bielski*, 1979]. In the course of our work we could find no evidence of any measurements of the trace metal content in KO$_2$. Recently [*Heller and Croot*, 2010a] we analyzed directly aliquots of KO$_2$ solutions for Fe and Cu and found that the KO$_2$ contained 0.7 ± 0.1 ppm Fe (dry weight) and no detectable Cu (less than 0.06 ppm Cu). Thus for the present work, using our standard protocol, we would have added ~3 pM Fe (<0.8 pM Cu) which would provide a maximum additional decay rate of 3 × 10^{-4} s^{-1} (using a reaction rate with Fe of 1 × 10^8 M^{-1} s^{-1}) significantly less than our observed rates. Thus the influence of trace metals in the KO$_2$ in our studies was apparently not significant to affect the results.

[17] 2. There is a significant amount of H$_2$O$_2$ in solutions prepared from KO$_2$ and this is unavoidable with any superoxide source, including photochemical and enzymatic production pathways. In the course of this work we came across problems with the current spectrophotometric methods used for calibrating O$_2^-$ that was generated photochemically using acetone or benzophenone in 2-propanol/water mixtures following the method of *McDowell et al.* [1983]. In brief the absorption spectra of acetone [*Feigenbrugel et al.*, 2005] and benzophenone [*Bennett and Johnston*, 1994] overlap with that of O$_2^-$ [*Bielski et al.*, 1985] and the reaction with benzophenone also produces acetone [*Görner*, 2006, 2007]. Similarly another common system used to generate a flux of O$_2^-$, Xanthine/Xanthine Oxidase also has been shown to be more complicated than first thought [*Hodges et al.*, 2000]. Thus in the present work we chose to use KO$_2$ as our source for O$_2^-$ in simple pulse chase decay experiments. In this work we always made measurements in order to determine the concentrations of both H$_2$O$_2$ and O$_2^-$ in each standard solution prepared, by UV spectrophotometry with either a LWCC-2100 100 cm path length liquid waveguide cell (World Precision Instruments, Sarasota, Florida), or a 10 cm Quartz-cuvette (Hellma), and an Ocean Optics USB4000 UV-VIS spectrophotometer combined with an Ocean Optics DT-MINI2-GS light source. Concentrations of H$_2$O$_2$ and O$_2^-$ were obtained by determining the least
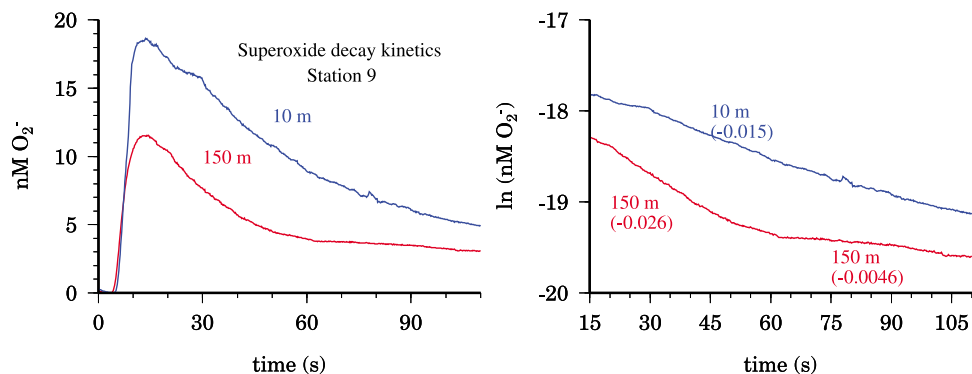
Figure 2. (left) Observed superoxide decay for diethylenetriaminepentaacetic acid (DTPA) amended seawater for two samples from Station 9. (right) Natural log transformed data of the superoxide decay rate in the left panel.

squares solution to the measured absorbance, at multiple wavelengths, by using published molar extinction coefficients for H_2O_2 [*Bielski and Allen*, 1977] and O_2^- [*Bielski et al.*, 1985]. A full description of this method can be found in our earlier work [*Heller and Croot*, 2010b]. Mean initial concentrations in the primary KO_2 solution assessed in this way were $900 \pm 50~\mu M$ for H_2O_2 and $90 \pm 10~\mu M$ O_2^-. No DTPA or other complexing agents were added to our KO_2 primary solution. H_2O_2 in the final seawater solutions was also assessed on occasion by using the chemiluminescence flow injection method [*Yuan and Shiller*, 1999] described above.

2.1.12. Effect of KO_2 Addition on pH of Samples

[18] In earlier works on superoxide kinetics in seawater, authors either did not report which pH scale they used or have used pH_{NBS}, apparently unaware of problems with this scale at high ionic strengths [*Dickson*, 1993; *Millero et al.*, 1993]. In the present work we are able to calculate the in situ and laboratory pH_{TOT} based on temperature, pressure, salinity, nutrient, alkalinity and TCO_2 data, provided by the TENATSO laboratory at the INDP in Cape Verde. Laboratory pH_{TOT} measurements were also made on the samples prior and after the addition of superoxide. In all cases pH_{TOT} increased after the addition of superoxide by approximately 0.08–0.10 pH_{TOT} units. These small increases in pH_{TOT} however did not apparently affect first-order decay rates in any significant manner as evidenced by the good precision for k_{obs} found over a range of superoxide additions (see section 2.1.10 on precision) where the maximal pH_{TOT} change was up to 0.20 pH units. It should be noted that a larger pH_{TOT} change was induced by the warming of the samples to the laboratory temperature and these temperature induced changes in superoxide reactivity need to be considered when considering in situ rates.

2.2. Calculation of Rate Data for Superoxide

[19] The raw chemiluminescence signal for the reaction between MCLA and O_2^- recorded by the computer was processed using a specially designed Labview^{TM} VI constructed for this purpose. Using standard kinetic fitting procedures, incorporating the nonlinear Levenberg-Marquardt algorithm [*Levenberg*, 1944; *Marquardt*, 1963], both the first- (in the following k_1 is equivalent to k_{obs}) and second-order (k_2) rates simultaneously (equation (3)). Previously

[*Heller and Croot*, 2010a] we have shown that equation (3) has the general solution:

$$[O_2^-] = \frac{k_1}{\left(\dfrac{k_1}{[O_2^-]_0} + k_2\right)e^{k_1 t} - k_2} \qquad (6)$$

Note that for the above equation when $k_2 = 0$ (no dismutation) the solution to equation (6) is the same as that for a normal first-order reaction. However, the equation does not collapse to solely second-order when $k_1 = 0$ because of the assumption made in the derivation that $k_1 \neq 0$. Thus in the case of $k_1 = 0$ the normal second-order rate equation should be used, for practical purposes in this work this was done when $k_1 < 1 \times 10^{-4}~s^{-1}$. Using the same reasoning the minimum value for k_1 (k_{obs}) that can be estimated using our approach is $1 \times 10^{-4}~s^{-1}$.

3. Results and Discussion

3.1. Vertical Profiles of Superoxide Organic Matter Kinetics

[20] Typical results for the O_2^- decay in DTPA amended seawater are shown in Figure 2 for two samples from different depths at S9. Both decay curves show the typical rapid decay of superoxide (initially ~100 nM) within the first 10 s before the sample has reached the detector. What is most interesting to note however is that the sample from 150 m displays two distinct decay rates (easily seen in the natural log transformed data), a fast initial rate for the first 60 s which is followed by an extremely slow decay, while the sample from 10 m only decays at an essentially constant rate. For the data from 150 m at S9 (Figure 2) we assessed changes in the first-order decay rate (k_{org}) over the course of the experiment, by analyzing the data over different time intervals. Using this approach it indicated that k_{org} in this sample reduced from 0.026 to 0.0046 s^{-1} over the course of the decay experiment. This change in the decay rate suggests either the appearance of a significant back reaction producing superoxide (see below) or alternatively that there were two pools of organic matter reacting with superoxide, a small highly reactive pool which was mostly responsible for the initial fast reaction rate and a larger less reactive group
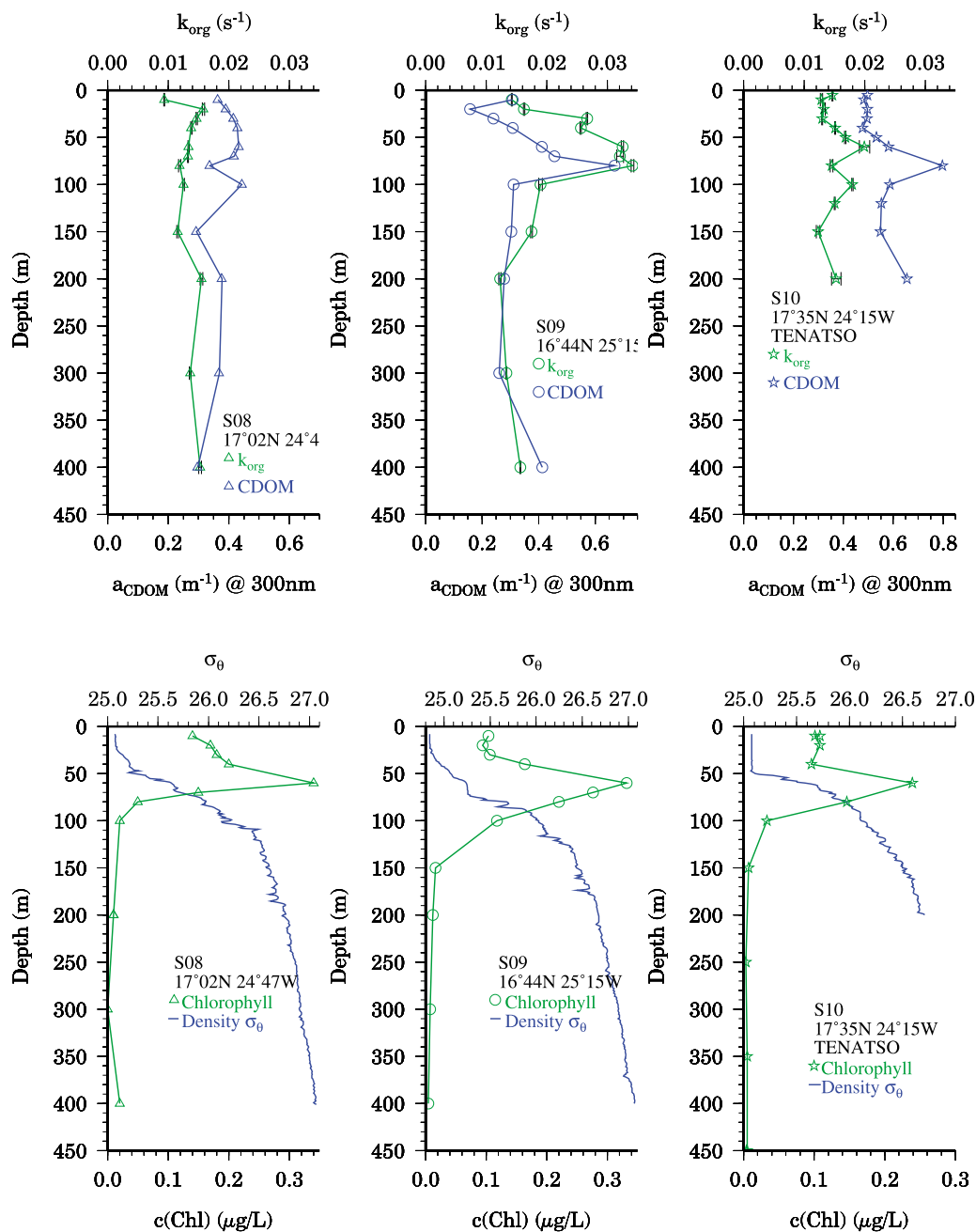
Figure 3. Vertical profiles of parameters measured in this study for three stations in the vicinity of Sao Vicente, Cape Verde. (top) Observed first-order O_2^- decay kinetics in seawater equilibrated with DTPA and colored dissolved organic matter (CDOM) absorbance (300 nm). (bottom) Vertical profiles of density anomaly (σ_θ) and chlorophyll. Error bars are shown for the 95% confidence interval.

of organic molecules that corresponded to the slower rate observed in the later part of the experiment. This change in the reaction rate with time was seen throughout the mid depth range (60–150 m) at S9, but was not apparent at S8 and S10.

[21] For the vertical profiles at S9 there was a clear maximum in k_{org} in the depth range 60–100 m which was below the mixed layer depth (MLD) but still within the euphotic zone (Figure 3). This maximum was not as distinct in the other two stations where decay rates were relatively uniform. Overall, with the exception of the samples men-

tioned above from S9, in every experiment the decay of O_2^- in DTPA amended seawater showed constant first-order decay kinetics with k_{org} ranging from 0.009 to 0.034 s^{-1} (Table 1), additionally for these samples the decay rate was found to not appreciably vary (less than 5%) as a function of the superoxide concentration (0–20 nM) suggesting that the reaction was not limited by the concentration of DOM or alternatively that a catalytic cycle with components of the DOM had been established.

[22] It is important that experimental data collected using nM concentrations of superoxide are fitted using
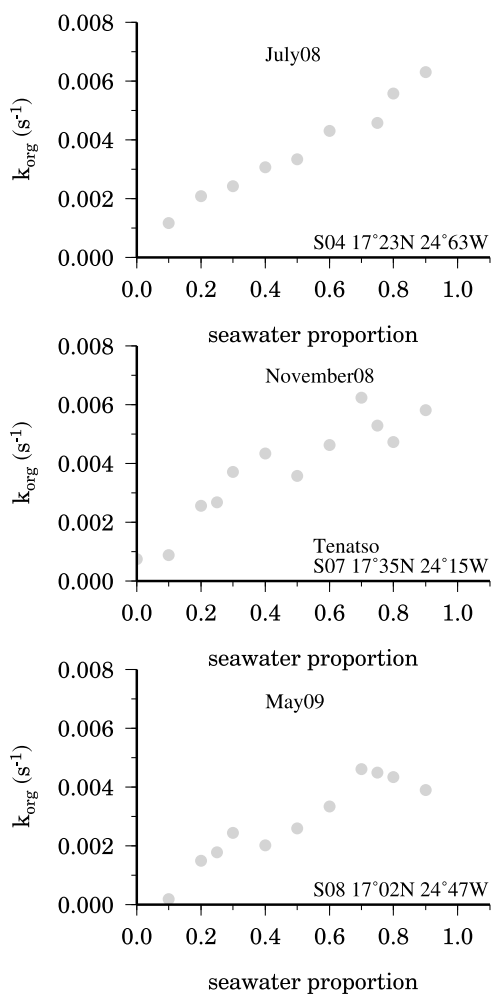
Figure 4. Variation in measured k_{org} for seawater diluted with Milli-Q from three near-surface samples collected during the period from July 2008 to May 2009.

equation (6) as this includes both the contribution of first-order and second decay processes (for more details, see *Heller and Croot* [2010a]). At the high values of k_{org} encountered in this study there is no statistically significant difference between a simple first-order fit and the method we use (Table 1). However, the inclusion of k_2 in general does improve the fit at high superoxide concentrations (>10 nM) or when $k_{org} \sim k_2[O_2^-]$.

3.2. Is There a Relationship Between CDOM and Superoxide Kinetics?

[23] In the present work we use values of $a_{CDOM(300)}$ as a proxy for DOM, as unfortunately we do not have any measurements of dissolved organic carbon (DOC) from these stations. Profiles of $a_{CDOM(300)}$ at S9 and S10 showed distinct maxima at 80 m just below the deep chlorophyll maxima (DCM) at 60 m (Figure 3) as has been observed previously in the tropical Atlantic [*Kitidis et al.*, 2006]. At S8 however $a_{CDOM(300)}$ was relatively uniform throughout the upper 400 m despite a well developed DCM at 60 m. Mixed layer depths (MLD, calculated as the depth at which σ_θ had increased by 0.05 over the surface value) at the time of sampling ranged from 27 m at S8, 33 m at S9, to 50 m at

S10 (Figure 2). For S10 the sampling was in the early morning when the MLD is at its deepest because of night-time convective cooling [*Brainerd and Gregg*, 1995]. Both S8 and S9 represent late afternoon stations when MLD are shallower. At all stations surveyed in May 2009 the DCM was below the MLD.

[24] CDOM is composed of an unknown number of potential chromophores [*Nelson and Siegel*, 2002] and forms only a small part of the DOC pool in the ocean, of which it is suggested to be a refractory component [*Nelson et al.*, 2007]. The sources of CDOM are not well described but include zooplankton and protozoan grazing [*Steinberg et al.*, 2004], bacterial production [*Nelson et al.*, 2004] and riverine input [*Blough and Del Vecchio*, 2002]. There are no major riverine sources in our study region [*Cotrim da Cunha et al.*, 2009] and our data strongly suggests that both the maxima in $a_{CDOM(300)}$ and k_{org} could be related to the remineralization of organic matter below the DCM via zooplankton grazing and bacterial activity.

[25] Previous work has suggested correlations between $a_{CDOM(300)}$ and (1) radical production via sunlight irradiation [*Dister and Zafiriou*, 1993; *O'Sullivan et al.*, 2005] and (2) superoxide decay in DTPA amended coastal seawater [*Goldstone and Voelker*, 2000]. The relationship between $a_{CDOM(300)}$ and radical production we cannot assess here directly as we did not examine production rates, however in the earlier study by *O'Sullivan et al.* [2005] the quantum yield of H_2O_2 was determined in the laboratory from photolysis of CDOM in natural water samples, including samples from rivers, estuaries, and both the coastal and open ocean. These authors found that the H_2O_2 quantum yield measured at 290 nm ranged from 4.2×10^{-4} in freshwater to 2.1×10^{-6} in marine waters and a linear relationship was found between the production of H_2O_2 and the loss of absorbance in the CDOM spectrum because of photobleaching. These authors also observed no significant relationship between H_2O_2 production and the dissolved organic carbon (DOC) concentration. However, samples which contained terrigeneous carbon in the form of humic substances showed a higher H_2O_2 production. In the context of the present work, Figure 3 indicates that there was potentially photobleaching occurring in the surface waters of S8 and S9 as evidenced by small decreases in $a_{CDOM(300)}$ values from depth toward the surface. No such gradient in $a_{CDOM(300)}$ is apparent at S10, however diel cycles may be important here, as S10 is the only station which was sampled in the morning after nighttime convective mixing could have eroded such a feature away.

[26] The correlation between $a_{CDOM(300)}$ and k_{org} found by *Goldstone and Voelker* [2000] for DTPA amended coastal seawater samples, predicts for our measured $a_{CDOM(300)}$ values, $k_{org} = 0.1$–0.2 s^{-1}, an order of magnitude more than what we observed (Table 1). Unlike the earlier coastal study, we found no statistically significant correlation between $a_{CDOM(300)}$ and k_{org} at any of the stations we sampled. This result strongly suggests that open ocean CDOM is significantly less reactive with superoxide than coastal waters and this may be related to the lack of riverine and terrestrial derived humic materials in open ocean waters. It also strongly suggests that the organic components reacting with superoxide in seawater make only minor contributions to $a_{CDOM(300)}$ in open ocean waters. To examine further the

Table 2. Reaction Rates of Organic Species Relevant to Seawater Involving O_2^{-} [a]

Reactant	Reaction	Rate M^{-1} s^{-1}	Reference
	Consumption of Superoxide		
1,4-benzoquinone	$Q + O_2^{-} \rightarrow Q^{\bullet -} + O_2$	8×10^8	*Meisel* [1975]
Hydroquinone	$QH_2 + O_2^{-} \rightarrow Q^{\bullet -} + H_2O_2$	1.7×10^7	*Rao and Hayon* [1975]
Glutathione	$GSH + O_2^{-} + H^{+} \rightarrow GS^{\bullet} + H_2O_2$	6.7×10^5	*Asada and Kanematsu* [1976]
Catechol	$Q(OH)_2 + O_2^{-} \rightarrow QO_2^{\bullet -} + H_2O_2$	2.7×10^5	*Bielski et al.* [1985]
	Production of Superoxide		
Semiquinone radical	$Q^{\bullet -} + O_2 \rightarrow Q + O_2^{-}$	5×10^4	*Eyer* [1991]
	Related Quinone/Hydroquinone Reactions		
Dismutation	$2Q^{\bullet -} \rightarrow Q + Q^{2-}$	2.3×10^7	*Meisel* [1975]

[a]Hydroquinone is a 1,4 diol and catechol is a 1,2 diol, both upon reaction with superoxide form their respective semiquinone radicals. Only compounds with reaction rate constants $>1 \times 10^5$ M^{-1} s^{-1} were considered here [*Bielski et al.*, 1985]; this then excludes amino acids, sugars, macronutrients and halides, all of which are critical constituents of seawater.

influence of CDOM/DOM on superoxide kinetics we routinely made a series of experiments with samples diluted with MQ, but using the same DTPA concentration, to check that the observed reaction was due to components in the seawater. In all cases the observed value of k_{org} varied linearly with the proportion of seawater in the sample (Figure 4), which when coupled with the assumption that DTPA complexation removed the reaction with trace metals, strongly suggests that it was an organic component of the seawater that was responsible for the observed first-order decay of superoxide. In all samples measured in our study we observed superoxide decay rates significantly in excess of that expected solely from the uncatalyzed dismutation reaction, the kinetics of which is well described from studies in pure water [*Bielski et al.*, 1985] and seawater [*Heller and Croot*, 2010a; *Zafiriou*, 1990].

[27] There are only a few open ocean studies of superoxide decay, our earlier study in the Southern Ocean [*Heller and Croot*, 2010a] found no significant organic mediated decay. Higher values ($k_{org} = 0.02 - 1.4$ s^{-1}) were found in coastal waters [*Goldstone and Voelker*, 2000] where DTPA was allowed to equilibrate with the seawater for several hours before analysis and a photochemical source of superoxide was used. The equilibration time with DTPA is a critical parameter to consider as we had previously observed in Southern Ocean samples [*Heller and Croot*, 2010a] that 2 h equilibration was insufficient to complex all metal reactions and that 12 h was optimal. A recent study in the tropical Pacific [*Rose et al.*, 2008] found values of 9.7×10^{-3} $s^{-1} > k > 1 \times 10^{-4}$ s^{-1}, but in this work DTPA was added immediately prior to measurement and an enzymatic source for superoxide was employed. This work is then difficult to compare with as the metal reactions are still included and problems also exist regarding the superoxide source. This is an important difference between our work and Rose et al. as enzymatic sources, with constant generation of superoxide, cannot be used in a simple pulse chase experiment such as performed in this work and instead must rely on the achievement of steady state conditions in order to calculate the decay rate from a production rate estimate.

3.3. What Organic Species Are Reacting With O_2^{-}?

[28] In the present work we have examined the relationship between DOM and superoxide decay kinetics with the initial assumption that CDOM is proportional to the reactive

organic component. Our results suggest that there is not a clear link between bulk CDOM and superoxide reactivity in open ocean waters. However, CDOM is obviously still critical for the photoproduction of superoxide [*Dister and Zafiriou*, 1993; *Micinski et al.*, 1993]. In this section we examine what organic species present in seawater may be responsible for the observed reactions with superoxide. Where rate constants are known for these reactions they are summarized in Table 2.

[29] Quinones are cellular components in bacteria [*Akagawa-Matsushita et al.*, 1992], marine fungi [*Bugni et al.*, 2000; *Son et al.*, 2002] and phytoplankton [*Greene et al.*, 1992; *Miller et al.*, 2009] which can be released to the water upon grazing or cell-lysis. There is currently increased interest in quinone/hydroquinone chemistry in natural waters because of their presence in humic and fulvic substances [*Miller et al.*, 2009; *Tossell*, 2009], where they may be responsible for much of the humic component in CDOM fluorescence [*Cory and McKnight*, 2005; *Klapper et al.*, 2002]. The possible impacts on biogeochemical cycles mediated by quinones was recently the subject of a review article [*Uchimiya and Stone*, 2009]. We could find no reports in the literature for the concentrations of quinones in the dissolved phase in seawater. Quinone like moieties have been detected in marine particles however [*Brandes et al.*, 2004] where they may contribute up to 10% of the particle content. Quinones may also be formed abiotically from reactions between proteins and carbohydrates in seawater [*Hedges*, 1978].

[30] Quinones react rapidly with superoxide (k_{R1} 1–9 × 10^8 M^{-1} s^{-1}) [*Bielski et al.*, 1985] and have been suggested previously to be the potential reactants in seawater [*Goldstone and Voelker*, 2000]. Using published data for the model quinone 1,4-benzoquinone ($k_{R1} = 1 \times 10^9$ M^{-1} s^{-1}, for reaction with superoxide) [*Meisel*, 1975], its semiquinone radical ($k_{R3} = 2.3 \times 10^7$ M^{-1} s^{-1}, self reaction) [*Meisel*, 1975] and hydroquinone ($k_{R2} = 1.7 \times 10^7$ M^{-1} s^{-1}, for reaction with superoxide)[*Rao and Hayon*, 1975] here we estimate, via simple numerical modeling incorporating the quinone reactions (R1)–(R4) described above and the uncatalyzed dismutation reaction for O_2^{-}, that a $k_{org} = 0.03$ s^{-1} would require a total quinone and hydroquinone concentration of ~9 nM for catalytic cycling under the conditions of our experiments. Note that the reaction between the semiquinone and superoxide is not included here as the reaction
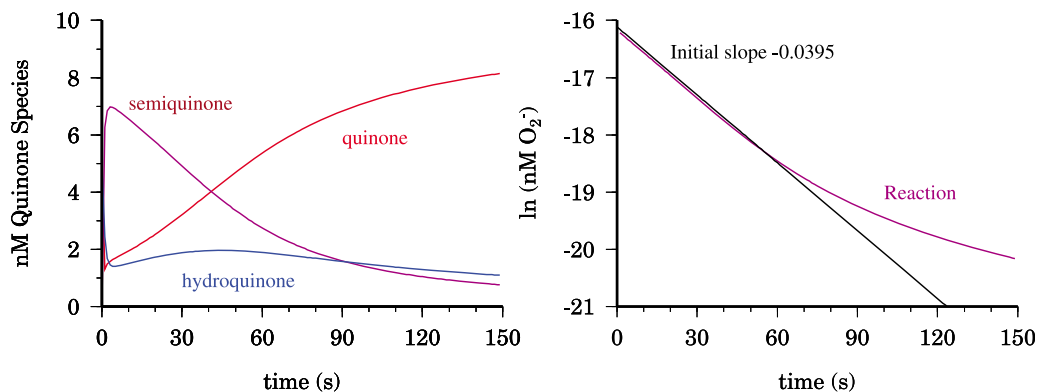
Figure 5. (left) Variation in the concentrations of quinone species as a function of time for a numerically simulated superoxide (100 nM) addition experiment. (right) Semilogarithimic plot of the superoxide decay in the same experiment; the initial decay rate is shown as a black line, and the overall decay is shown as a purple line. In this experiment the initial conditions were 5 nM quinone plus 5 nM hydroqui-none, though experiments initialized with 10 nM quinone or 10 nM hydroquinone gave almost identical results after 5 s of simulated reaction time.

rate constant is presently unknown, however previous work suggests that it does not influence the overall reaction kinetics significantly [*Ishii and Fridovich*, 1990; *Roginsky and Barsukova*, 2000]. The reaction between the hydro-quinone and O_2 is also neglected as it is slow because of it being spin forbidden [*Roginsky and Barsukova*, 2000].

[31] Figure 5 illustrates the results for a numerical simulation of the reaction between 10 nM of quinone/hydroquinone and 100 nM of superoxide using the reaction rates mentioned above. It is clear from Figure 5 that the decay rate is first-order over the first 60 s but then slows as the production of superoxide from the semiquinone reaction with oxygen begins to become more important when superoxide drops below ~10 nM. The modeled result is similar to what was observed in Figure 2 for the sample from S9 at 150 m, hinting that reactions with quinones may have been important there. The critical reactions involved

are the rate of regeneration of superoxide from the reaction between oxygen and the semiquinone radical ($k_{R4} = 5 \times 10^4$ M^{-1} s^{-1}) [*Eyer*, 1991] and the dismutation rate of the radical into the quinone and the hydroquinone ($k_{R2} = 2.3 \times 10^7$ M^{-1} s^{-1}). This also helps to explain why there was no apparent relationship between k_{org} with CDOM absorbance as at a concentration of 10 nM of the quinone no relationship with CDOM absorbance should be expected as the contri-bution of the quinone to the CDOM absorbance is on the order of 0.5 to 1%. This is based on a typical molar absorptivity of 2500 M^{-1} cm^{-1} at 290 nm for the hydro-quinone and significantly less for the quinone; thus with a 1m path length this corresponds to an absorbance of 0.0025 when the overall absorbance is 0.3 to 0.6 as seen in Figure 3.

[32] Using our values for k_{org} and compilations of O_2^- reaction rates with organic compounds [*Bielski et al.*, 1985; *Shkarina et al.*, 2001] we can draw up a list of alternative
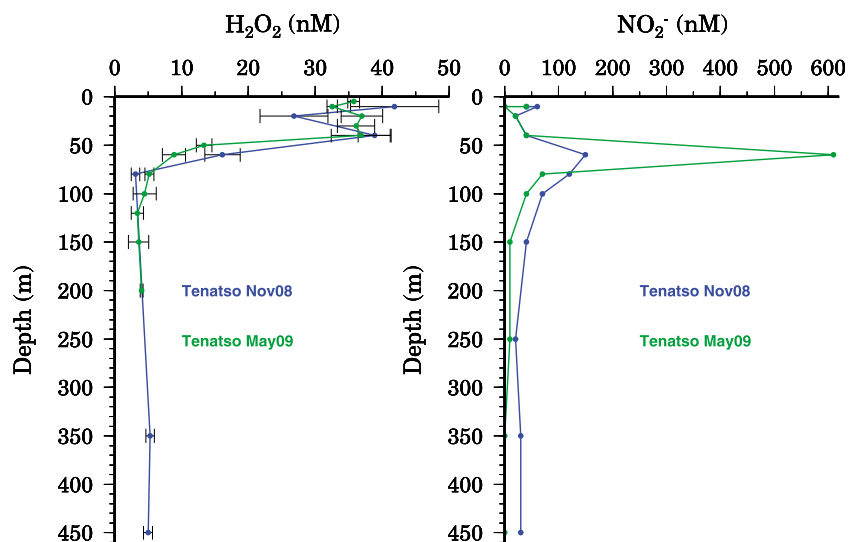

Figure 6. (left) H_2O_2 and (right) nitrite vertical profiles from TENATSO (17°35′N, 24°15′W). Error bars are shown for the 95% confidence interval.
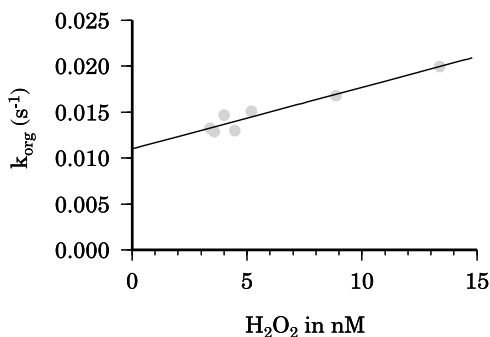
Figure 7. The linear relationship between k_{org} and H_2O_2 for waters below the mixed layer at the TENATSO site in May 2009.

organic compounds that could also be responsible for the observed reaction kinetics (Table 2). Of all the candidate molecules, the quinones as discussed above are still the most likely. Two candidates do stand out as having some small influence on the observed rates. Glutathione and related thiols react rapidly with superoxide ($k = 6.7 \times 10^5$ M^{-1} s^{-1}) [*Asada and Kanematsu*, 1976] but so far have been only found at sub nM concentrations in seawater [*Dupont et al.*, 2006]. Catechols ($k = 2.7 \times 10^5$ M^{-1} s^{-1}) may be present in seawater at low nM levels as siderophores [*Butler*, 2005] and can be further oxidized to quinones. Currently however there is no information on the concentrations of quinones, catechols or thiols in the waters around Cape Verde and so no firm conclusions can be drawn on the identification of the organic species reacting with superoxide.

3.4. Superoxide Kinetics and H_2O_2 Production at TENATSO

[33] At the TENATSO site (S10) surface concentrations of nitrate and phosphate were at trace levels in the mixed layer, below which the nutricline appeared along with a distinct nitrite maximum at 60 m (Figure 6) coincident with the DCM (Figure 3). In both November 2008 and May 2009, H_2O_2 was relatively constant in the upper 50 m and decreased rapidly below (Figure 6) consistent with previous data from this region [*Croot et al.*, 2004; *Steigenberger and Croot*, 2008]. Both the H_2O_2 and nitrite profiles show the importance of photochemistry on the distribution of these species in the water column, but also show the contrast between the species in terms of photoproduction (H_2O_2) and photodecay (Nitrite).

[34] Interestingly there was a strong correlation between H_2O_2 concentrations and k_{org} for samples below the MLD ($R^2 = 0.93$, n = 7, Figure 7) away from the main photo-production zone for H_2O_2. This raises the intriguing possibility that if quinones are determining k_{org} then the relationship to H_2O_2 in deep waters may be due to the back reaction between O_2 and the semiquinone radical producing superoxide (R4) which in turn can react via a number of pathways, including reaction with hydroquinone, to produce H_2O_2 (R2). The reaction scheme outlined is in essence the same as that for the autoxidation of hydroquinones [*Eyer*, 1991; *Ishii and Fridovich*, 1990] and could be responsible for part of the observed deep water H_2O_2 production that maintains the low concentrations observed there [*Yuan and*

Shiller, 2004]. Repeating the numerical modeling performed above for the O_2^- decay experiments in the presence of quinones, but in the absence of an external O_2^- source, suggests that a constant production rate of 1 nM per day of H_2O_2 can be generated using only the catalytic action of 2 nM hydroquinone and a steady state O_2^- concentration of 0.65 pM resulting from the reaction between O_2 and the semiquinone radical. This model result is however clearly a simplification as reactions with trace metals are most likely also important in the deep waters and they potentially may accelerate reactions forming H_2O_2 directly [*Li and Trush*, 1993] but also may reduce the O_2^- steady state concentration[*Heller and Croot*, 2010a]. Further work is therefore necessary to elucidate the role of quinones within DOM and their potential role in redox cycling in the ocean. The use of fluorescence techniques to quantify the quinone content of CDOM [*Cory and McKnight*, 2005] appears a promising method for application to marine studies.

4. Conclusions

[35] In tropical Atlantic waters we observed significant reactions for superoxide with organic matter in the upper water column. Vertical profiles of k_{org} were similar to, but not identical to, profiles of $a_{CDOM(300)}$. At one station maxima for k_{org} were found just below the chlorophyll maximum, suggesting that this pattern may be due to the production or release of unbleached organic matter. Following up on earlier suggestions that the superoxide reactive component of CDOM may comprise quinone functional groups, exudated from bacteria or phytoplankton, our results indicate that nM concentrations of dissolved quinones could be responsible for the observed k_{org} values. Though there is currently no data on quinones in seawater to confirm this. Our work highlights a poorly understood process which impacts on the biogeochemical cycling of CDOM, H_2O_2 and trace metals in the open ocean.

References

Akagawa-Matsushita, M., T. Itoh, Y. Katayama, H. Kuraishi, and K. Yamasato (1992), Isoprenoid quinone composition of some marine alteromonas, marinomonas, deleya, pseudomonas and shewanella species, *J. Gen. Microbiol.*, *138*, 2275–2281.

Akutsu, K., H. Nakajima, T. Katoh, S. Kino, and K. Fujimori (1995), Chemiluminescence of *Cipridina* luciferin analogs. 2. Kinetic studies on the reaction of 2-methyl-6-phenylimidazo[1,2-*a*]pyrazin-3(7*H*)-one (CLA) with superoxide: Hydroperoxyl radical is an actual active species used to initiate the reaction, *J. Chem. Soc., Perkin Trans.*, *2*, 1699–1706.

Asada, K., and S. Kanematsu (1976), Reactivity of thiols with superoxide radicals, *Agric. Biol. Chem.*, *40*(9), 1891–1892.

Bennett, G. E., and K. P. Johnston (1994), UV-visible absorbency spectroscopy of organic probes in supercritical water, *J. Phys. Chem.*, *98*(2), 441–447, doi:10.1021/j100053a017.

Bielski, B. H. J., and A. O. Allen (1977), Mechanism of the disproportionation of superoxide radicals, *J. Phys. Chem.*, *81*(11), 1048–1050, doi:10.1021/j100526a005.

Bielski, B. H. J., D. E. Cabelli, R. L. Arudi, and A. B. Ross (1985), Reactivity of HO_2/O_2^- radicals in aqueous solution, *J. Phys. Chem. Ref. Data*, *14*(4), 1041–1100.

Blough, N. V., and R. Del Vecchio (2002), Chromophoric DOM in the coastal ocean, in *Biogeochemistry of Marine Dissolved Organic Matter*, edited by D. A. Hansell and C. A. Carlson, pp. 509–546, Academic, San Diego, Calif., doi:10.1016/B978-012323841-2/50012-9.

Brainerd, K. E., and M. C. Gregg (1995), Surface mixed and mixing layer depths, *Deep Sea Res., Part I*, 42, 1521–1543, doi:10.1016/0967-0637 (95)00068-H.

Brandes, J. A., C. Lee, S. Wakeham, M. Peterson, C. Jacobsen, S. Wirick, and G. Cody (2004), Examining marine particulate organic matter at submicron scales using scanning transmission X-ray microscopy and carbon X-ray absorption near edge structure spectroscopy, *Mar. Chem.*, 92(1–4), 107–121, doi:10.1016/j.marchem.2004.06.020.

Bugni, T. S., D. Abbanat, V. S. Bernan, W. M. Maiese, M. Greenstein, R. M. Van Wagoner, and C. M. Ireland (2000), Yanuthones: Novel metabolites from a marine isolate of *Aspergillus niger*, *J. Org. Chem.*, 65(21), 7195–7200, doi:10.1021/jo0006831.

Butler, A. (2005), Marine siderophores and microbial iron mobilization, *Biometals*, 18(4), 369–374, doi:10.1007/s10534-005-3711-0.

Cory, R. M., and D. M. McKnight (2005), Fluorescence Spectroscopy Reveals Ubiquitous Presence of Oxidized and Reduced Quinones in Dissolved Organic Matter, *Environ. Sci. Technol.*, 39(21), 8142–8149, doi:10.1021/es0506962.

Cory, R. M., J. B. Cotner, and K. McNeill (2008), Quantifying interactions between singlet oxygen and aquatic fulvic acids, *Environ. Sci. Technol.*, 43(3), 718–723, doi:10.1021/es801847g.

Cotrim da Cunha, L., P. Croot, and J. LaRoche (2009), Influence of river discharge in the tropical and subtropical North Atlantic Ocean, *Limnol. Oceanogr.*, 54(2), 644–648.

Croot, P. L., P. Streu, I. Peeken, K. Lochte, and A. R. Baker (2004), Influence of the ITCZ on H_2O_2 in near surface waters in the equatorial Atlantic Ocean, *Geophys. Res. Lett.*, 31, L23S04, doi:10.1029/2004GL000154.

Dickson, A. G. (1993), pH buffers for sea water media based on the total hydrogen ion concentration scale, *Deep Sea Res., Part I*, 40(1), 107–118, doi:10.1016/0967-0637(93)90055-8.

Dister, B., and O. C. Zafiriou (1993), Photochemical free radical production rates in the eastern Caribbean, *J. Geophys. Res.*, 98(C2), 2341–2352, doi:10.1029/92JC02765.

Dupont, C. L., J. W. Moffett, R. R. Bidigare, and B. A. Ahner (2006), Distributions of dissolved and particulate biogenic thiols in the subartic Pacific Ocean, *Deep Sea Res., Part I*, 53(12), 1961–1974, doi:10.1016/j.dsr.2006.09.003.

Eyer, P. (1991), Effects of superoxide dismutase on the autoxidation of 1,4-hydroquinone, *Chem. Biol. Interact.*, 80(2), 159–176, doi:10.1016/0009-2797(91)90022-Y.

Feigenbrugel, V., C. Loew, S. Le Calve, and P. Mirabel (2005), Near-UV molar absorptivities of acetone, alachlor, metolachlor, diazinon and dichlorvos in aqueous solution, *J. Photochem. Photobiol. Chem.*, 174(1), 76–81, doi:10.1016/j.jphotochem.2005.03.014.

Fujimori, K., H. Nakajima, K. Akutsu, M. Mitani, H. Sawada, and M. Nakayama (1993), Chemiluminescence of *Cypridina* luciferin analogs. Part 1. Effect of pH on rates of spontaneous autoxidation of CLA in aqueous buffer solutions, *J. Chem. Soc., Perkin Trans.*, 2(12), 2405–2409.

Fujimori, K., T. Komiyama, H. Tabata, T. Nojima, K. Ishiguro, Y. Sa-waki, H. Tatsuzawa, and M. Nakano (1998), Chemiluminescence of *Cypridina* luciferin analogs. Part 3. MCLA chemiluminescence with singlet oxygen generated by the retro-Diels-Alder reaction of a naphthalene endoperoxide, *Photochem. Photobiol.*, 68(2), 143–149, doi:10.1111/j.1751-1097.1998.tb02481.x.

Goldstone, J. V., and B. M. Voelker (2000), Chemistry of superoxide radical in seawater: CDOM associated sink of superoxide in coastal waters, *Environ. Sci. Technol.*, 34, 1043–1048, doi:10.1021/es9905445.

Görner, H. (2006), Oxygen uptake and involvement of superoxide radicals upon photolysis of ketones in air-saturated aqueous alcohol, formate, amine or ascorbic acid solutions, *Photochem. Photobiol.*, 82(3), 801–808, doi:10.1562/2005-12-06-RA-746.

Görner, H. (2007), Oxygen uptake upon photolysis of 3-benzoylpyridine and 3,3 '-dipyridylketone in air-saturated aqueous solution in the presence of formate, ascorbic acid, alcohols and amines, *J. Photochem. Photobiol. Chem.*, 187(1), 105–112, doi:10.1016/j.jphotochem.2006.09.018.

Gotoh, N., and E. Niki (1990), Rate of spin-trapping of superoxide as studied by chemiluminescence, *Chem. Lett.*, 19(8), 1475–1478, doi:10.1246/cl.1990.1475.

Grasshoff, K., K. Kremling, and M. Ehrhardt (1999), *Methods of Seawater Analysis*, John Wiley, Weinheim, Germany, doi:10.1002/9783527613984.

Greene, R. M., R. J. Geider, Z. Kolber, and P. G. Falkowski (1992), Iron-induced changes in light harvesting and photochemical energy conversion processes in eukaryotic marine algae, *Plant Physiol.*, 100, 565–575, doi:10.1104/pp.100.2.565.

Hedges, J. I. (1978), The formation and clay mineral reactions of melanoidins, *Geochim. Cosmochim. Acta*, 42(1), 69–76, doi:10.1016/0016-7037(78)90218-1.

Heller, M. I., and P. L. Croot (2010a), Superoxide decay kinetics in the Southern Ocean, *Environ. Sci. Technol.*, 44(1), 191–196, doi:110.1021/es901766r.

Heller, M. I., and P. L. Croot (2010b), Application of a superoxide (O_2^-) thermal source (SOTS-1) for the determination and calibration of O_2^- fluxes in seawater, *Anal. Chim. Acta*, 667, 1–13, doi:10.1016/j.aca.2010.03.054.

Hodges, G. R., M. J. Young, T. Paul, and K. U. Ingold (2000), How should xanthine oxidase-generated superoxide yields be measured?, *Free Radic. Biol. Med.*, 29(5), 434–441, doi:10.1016/S0891-5849(00)00298-7.

Ishii, T., and I. Fridovich (1990), Dual effects of superoxide-dismutase on the autoxidation of 1,4-naphthohydroquinone, *Free Radic. Biol. Med.*, 8(1), 21–24, doi:10.1016/0891-5849(90)90140-E.

Kambayashi, Y., and K. Ogino (2003), Reestimation of *Cypridina* lueciferin analogs (MCLA) as a chemiluminescence probe to detect active oxygen species-cautionary note for use of MCLA, *J. Toxicol. Sci.*, 28(3), 139–148, doi:10.2131/jts.28.139.

Kitidis, V., A. P. Stubbins, G. Uher, R. C. Upstill Goddard, C. S. Law, and E. M. S. Woodward (2006), Variability of chromophoric organic matter in surface waters of the Atlantic Ocean, *Deep Sea Res., Part II*, 53(14–16), 1666–1684, doi:10.1016/j.dsr2.2006.05.009.

Klapper, L., D. M. McKnight, J. R. Fulton, E. L. Blunt-Harris, K. P. Nevin, D. R. Lovley, and P. G. Hatcher (2002), Fulvic acid oxidation state detection using fluorescence spectroscopy, *Environ. Sci. Technol.*, 36(14), 3170–3175, doi:10.1021/es0109702.

Levenberg, K. (1944), A method for the solution of certain non-linear problems in least squares, *Q. Appl. Math.*, 2, 164–168.

Li, Y. B., and M. A. Trush (1993), Oxidation of hydroquinone by copper: Chemical mechanism and biological effects, *Arch. Biochem. Biophys.*, 300(1), 346–355, doi:10.1006/abbi.1993.1047.

Marquardt, D. W. (1963), An algorithm for least-squares estimation of nonlinear parameters, *SIAM J. Appl. Math.*, 11(2), 431–441, doi:10.1137/0111030.

Marshall, J. A., M. de Salas, T. Oda, and G. Hallegraeff (2005), Superoxide production by marine microalgae, *Mar. Biol. Berlin*, 147(2), 533–540, doi:10.1007/s00227-005-1596-7.

McDowell, M. S., A. Bakac, and J. H. Espenson (1983), A convenient route to superoxide ion in aqueous solution, *Inorg. Chem.*, 22(5), 847–848, doi:10.1021/ic00147a033.

Meisel, D. (1975), Free energy correlation of rate constants for electron transfer between organic systems in aqueous solutions, *Chem. Phys. Lett.*, 34(2), 263–266, doi:10.1016/0009-2614(75)85269-9.

Micinski, E., L. A. Ball, and O. C. Zafiriou (1993), Photochemical oxygen activation: Superoxide radical detection and production rates in the eastern Caribbean, *J. Geophys. Res.*, 98(C2), 2299–2306, doi:10.1029/92JC02766.

Miller, M. P., D. M. McKnight, and S. C. Chapra (2009), Production of microbially derived fulvic acid from photolysis of quinone-containing extracellular products of phytoplankton, *Aquat. Sci.*, 71(2), 170–178, doi:10.1007/s00027-009-9194-2.

Millero, F. J., J. Z. Zhang, S. Fiol, S. Sotolongo, R. N. Roy, K. Lee, and S. Mane (1993), The use of buffers to measure the pH of seawater, *Mar. Chem.*, 44(2–4), 143–152, doi:10.1016/0304-4203(93)90199-X.

Mitani, M., Y. Yokoyama, S. Ichikawa, H. Sawada, T. Matsumoto, K. Fujimori, and M. Kosugi (1994), Determination of horseradish-peroxidase concentration using the chemiluminescence of *Cypridina* luciferin analog, 2-Methyl-6-(P-methyoxyphenyl)-3,7-dihydroimidazo [1,2-A]pyrazin-3-one, *J. Biolumin. Chemilumin.*, 9(6), 355–361, doi:10.1002/bio.1170090602.

Nelson, N. B., and D. A. Siegel (2002), Chromophoric DOM in the open ocean, in *Biogeochemistry of Marine Dissolved Organic Matter*, edited by D. A. Hansell and C. A. Carlson, pp. 547–578, Academic, San Diego, Calif., doi:10.1016/B978-012323841-2/50013-0.

Nelson, N. B., C. A. Carlson, and D. K. Steinberg (2004), Production of chromophoric dissolved organic matter by Sargasso Sea microbes, *Mar. Chem.*, 89(1–4), 273–287, doi:10.1016/j.marchem.2004.02.017.

Nelson, N. B., D. A. Siegel, C. A. Carlson, C. Swan, J. W. M. Smethie, and S. Khatiwala (2007), Hydrography of chromophoric dissolved organic matter in the North Atlantic, *Deep Sea Res., Part I*, 54(5), 710–731, doi:10.1016/j.dsr.2007.02.006.

O'Sullivan, D. W., P. J. Neale, R. B. Coffin, T. J. Boyd, and S. L. Osburn (2005), Photochemical production of hydrogen peroxide and methylhydroperoxide in coastal waters, *Mar. Chem.*, 97(1–2), 14–33, doi:10.1016/j.marchem.2005.04.003.

Rao, P. S., and E. Hayon (1975), Redox potentials of free radicals. IV. Superoxide and hydroperoxy radicals · O_2^- and · HO_2, *J. Phys. Chem.*, *79*(4), 397–402, doi:10.1021/j100571a021.

Roginsky, V., and T. Barsukova (2000), Kinetics of oxidation of hydroquinones by molecular oxygen: Effect of superoxide dismutase, *J. Chem. Soc., Perkin Trans.*, *2*, 1575–1582, doi:10.1039/b000538j.

Roginsky, V. A., L. M. Pisarenko, W. Bors, and C. Michel (1999), The kinetics and thermodynamics of quinone-semiquinone-hydroquinone systems under physiological conditions, *J. Chem. Soc., Perkin Trans.*, *2*(4), 871–876.

Rose, A. L., and D. Waite (2006), Role of superoxide in the photochemical reduction of iron in seawater, *Geochim. Cosmochim. Acta*, *70*(15), 3869–3882, doi:10.1016/j.gca.2006.06.008.

Rose, A. L., E. A. Webb, T. D. Waite, and J. W. Moffett (2008), Measurement and implications of nonphotochemically generated superoxide in the equatorial Pacific Ocean, *Environ. Sci. Technol.*, *42*(7), 2387–2393, doi:10.1021/es7024609.

Scott, D. T., D. M. McKnight, E. L. Blunt-Harris, S. E. Kolesar, and D. R. Lovley (1998), Quinone moieties act as electron acceptors in the reduction of humic substances by humics-reducing microorganisms, *Environ. Sci. Technol.*, *32*(19), 2984–2989, doi:10.1021/es980272q.

Shkarina, E. I., T. V. Makisimova, I. N. Nikulina, E. L. Lozovskaya, Z. V. Chumakova, V. P. Pakhomov, I. I. Sapezhinskii, and A. P. Azamastsev (2001), Effect of biologically active substances on the antioxidant activity of phytopreparations, *Pharm. Chem. J.*, *35*, 333–340, doi:10.1023/A:1012349806071.

Son, B., J. Kim, H. Choi, and J. Kang (2002), A radical scavenging Farnesylhydroquinone from a marine-derived fungus *Penicillium* sp., *Arch. Pharm. Res.*, *25*(1), 77–79, doi:10.1007/BF02975266.

Steigenberger, S., and P. L. Croot (2008), Identifying the processes controlling the distribution of H_2O_2 in surface waters along a meridional transect in the eastern Atlantic, *Geophys. Res. Lett.*, *35*, L03616, doi:10.1029/2007GL032555.

Steinberg, D. K., N. B. Nelson, C. A. Carlson, and A. C. Prusak (2004), Production of chromophoric dissolved organic matter (CDOM) in the open ocean by zooplankton and the colonial cyanobacterium *Trichodesmium* spp., *Mar. Ecol. Prog. Ser.*, *267*, 45–56, doi:10.3354/meps267045.

Tossell, J. A. (2009), Quinone-hydroquinone complexes as model components of humic acids: Theoretical studies of their structure, stability and Visible-UV spectra, *Geochim. Cosmochim. Acta*, *73*(7), 2023–2033, doi:10.1016/j.gca.2008.12.029.

Uchimiya, M., and A. T. Stone (2009), Reversible redox chemistry of quinones: Impact on biogeochemical cycles, *Chemosphere*, *77*(4), 451–458, doi:10.1016/j.chemosphere.2009.07.025.

Voelker, B. M., D. L. Sedlak, and O. C. Zafiriou (2000), Chemistry of superoxide radical in seawater: Reactions with organic Cu complexes, *Environ. Sci. Technol.*, *34*, 1036–1042, doi:10.1021/es990545x.

Weinstein, J., and B. H. J. Bielski (1979), Kinetics of the interaction of HO_2 and O_2^- radicals with hydrogen peroxide. The Haber-Weiss reaction, *J. Am. Chem. Soc.*, *101*, 58–62, doi:10.1021/ja00495a010.

Yuan, J., and A. M. Shiller (1999), Determination of subnanomolar levels of hydrogen peroxide in seawater by reagent-injection chemiluminescence detection, *Anal. Chem.*, *71*, 1975–1980, doi:10.1021/ac981357c.

Yuan, J., and A. M. Shiller (2001), The distribution of hydrogen peroxide in the southern and central Atlantic Ocean, *Deep Sea Res., Part II*, *48*, 2947–2970, doi:10.1016/S0967-0645(01)00026-1.

Yuan, J., and A. M. Shiller (2004), Hydrogen peroxide in deep waters of the North Pacific Ocean, *Geophys. Res. Lett.*, *31*, L01310, doi:10.1029/2003GL018439.

Zafiriou, O. C. (1990), Chemistry of superoxide ion (O_2^-) in seawater. I. pK_{asw}* (HOO) and uncatalysed dismutation kinetics studied by pulse radiolysis, *Mar. Chem.*, *30*, 31–43, doi:10.1016/0304-4203(90)90060-P.

Zafiriou, O. C., B. M. Voelker, and D. L. Sedlak (1998), Chemistry of the superoxide radical (O_2^-) in seawater: Reactions with inorganic copper complexes, *J. Phys. Chem. A*, *102*(28), 5693–5700, doi:10.1021/jp980709g.

Zheng, J., S. R. Springston, and J. Weinstein-Lloyd (2003), Quantitative analysis of hydroperoxyl radical using flow injection analysis with chemiluminescence detection, *Anal. Chem.*, *75*(17), 4696–4700, doi:10.1021/ac034429v.

P. L. Croot and M. I. Heller, FB2 Marine Biogeochemie, Leibniz-Institut für Meereswissenschaften, Dienstgebäude Westufer, Düsternbrooker Weg 20, D-24105 Kiel, Germany. (pcroot@ifm-geomar.de)